

## Use of the $(\gamma, \gamma')$ Reaction for Studying the Energy Levels of $^{139}\text{La}$

R. Moreh and A. Nof

*Nuclear Research Centre, Negev, Beer Sheva, Israel*

(Received 24 July 1970)

Elastic and inelastic scattering of monochromatic photons were used for studying nuclear energy levels in  $^{139}\text{La}$ ; the photons were produced by thermal-neutron capture in titanium and iron. Two independent resonance lines at 6418 and 6760 keV were excited with the titanium  $\gamma$  source, and three independent resonances at 6018, 7279, and 7632 keV were excited with the iron  $\gamma$  source. Some 18 known low-lying levels were populated by deexcitation of these resonance levels. The angular distribution of some intense elastic and inelastic lines were measured and the following spin and parity determinations (keV,  $J^\pi$ ) were made: 166,  $\frac{5}{2}^-$ ; 1220,  $\frac{5}{2}^-, (\frac{3}{2}^-)$ ; 1384,  $\frac{1}{2}^-$ ; 1419,  $\frac{7}{2}^-, (\frac{4}{2}^-)$ ; 1536,  $\frac{7}{2}^-$ ; 1580,  $\frac{3}{2}^-$ ; 2232,  $(\frac{1}{2}^-, \frac{11}{2}^-)$ ; 6018,  $\frac{7}{2}^-$ ; 6418,  $\frac{3}{2}^-$ ; and 6760,  $\frac{7}{2}^-$ , where parentheses denote uncertainties. The parities of the 6018- and 6418-keV levels were directly determined using a Compton polarimeter. The total radiative widths of the 6018- and 6418-keV levels were measured and found to be  $\Gamma_\gamma = 0.051$  and  $0.081$  eV, respectively. The  $^{139}\text{La}$  levels are compared with recent theoretical calculations.

### I. INTRODUCTION

In the present work, the low-energy levels of  $^{139}\text{La}$  were investigated using  $\gamma$  sources obtained from thermal-neutron capture in iron and titanium. The same technique was employed in previous publications<sup>1-3</sup> to study low-lying energy levels in  $^{141}\text{Pr}$ ,  $^{205}\text{Tl}$ , and  $^{75}\text{As}$ , and the potentialities and limitations of this method were discussed in some detail. This method was also used by other investigators for studying low-lying levels in  $^{62}\text{Ni}$ ,  $^{112}\text{Cd}$ ,  $^{130}\text{Te}$ , and  $^{66}\text{Zn}$ .<sup>4-8</sup>

It should be realized that the choice of the target in the present technique is conditioned by the fact that a random overlap should exist between at least one of the incident capture  $\gamma$  lines and a level in  $^{139}\text{La}$ . It turned out that three iron capture  $\gamma$  lines happened to overlap three levels in  $^{139}\text{La}$  of which only one level was strongly excited. In the case of the titanium  $\gamma$  source, two resonance levels in  $^{139}\text{La}$  were excited. It was thus possible to establish the spins, parities, and decay properties of some of these resonance states and the spins of some low-lying levels strongly populated by transitions from these resonances. The spins were determined by angular-distribution measurements, and the parities by polarization measurements. The widths of some of the resonance levels were measured using self-absorption, temperature variation, and absolute scattering-cross-section measurements.

It should be noted that, in general, new low-lying levels may be deduced using the  $(\gamma, \gamma')$  technique; this is done by relying on the assumption that strong high-energy  $\gamma$  rays are emitted in primary transitions. Nevertheless, no attempt was made in the present work to deduce new levels, be-

cause of the ambiguity in associating a given  $\gamma$  transition with a specific resonance level. This ambiguity may be resolved, in principle, by coincidence measurements between Ge(Li) and NaI detectors. This implies very long running times which were impracticable in the present work. It was thus decided to study in detail only transitions to known low-lying levels in  $^{139}\text{La}$ , as will be seen later.

The  $^{139}\text{La}$  level were studied previously by several authors. These studies were made using the  $(n, n'\gamma)$  reaction,<sup>9,10</sup> the  $(n, n')$  reaction,<sup>11</sup> the  $\beta$  decay of  $^{139}\text{Ba}$ ,<sup>12,13</sup> the  $^{138}\text{Ba}(^3\text{He}, d)$  reaction,<sup>14</sup> and the  $(\gamma, \gamma')$  reaction.<sup>15</sup> The position of several levels were thus determined and the  $J^\pi$  values of some levels were assigned. A preliminary report of some of the results of the present work was published earlier.<sup>16</sup>

### II. EXPERIMENTAL PROCEDURE

The  $\gamma$  sources were obtained by thermal-neutron capture in Ti and Fe disks which were placed near the reactor core along a horizontal tangential beam tube of the IRR-2 reactor. Details of the experimental arrangement and the scattering system were described in a previous publication.<sup>1</sup>

Typical  $\gamma$  intensities were of the order of  $10^8$  monoenergetic photons/cm<sup>2</sup>sec on the target scatterer. The scattered radiation spectrum was observed by placing a 10-gm/cm<sup>2</sup>-thick lanthanum target of 11-cm diam. The detectors used were either a 5-in.  $\times$  5-in. NaI crystal or Ge(Li) coaxial crystals of volume 10 and 20 cc. The pulses from the Ge(Li) detector were passed to an ORTEC pre-amplifier, biased amplifier system, then a base-line restorer, and accumulated in a 1024-channel

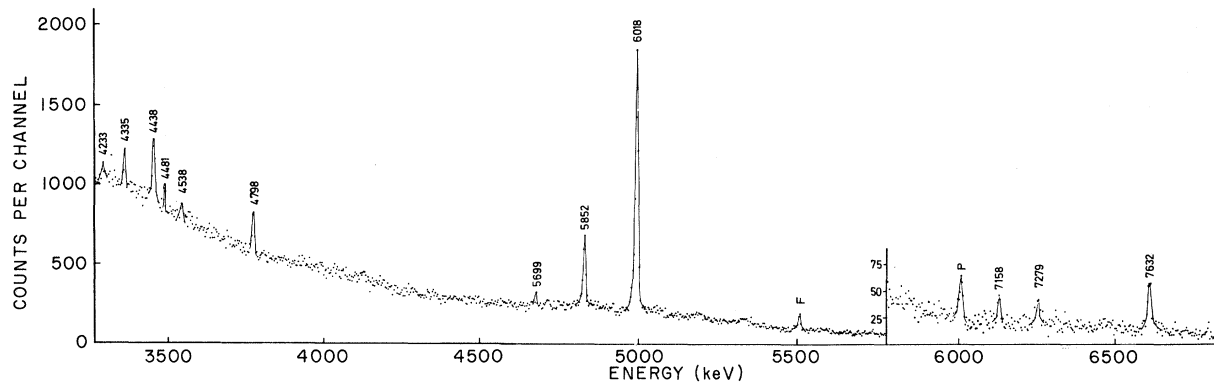


FIG. 1. Scattered  $\gamma$  spectrum from a La target at an angle of  $135^\circ$  measured by a 10-cc detector. The  $\gamma$  source was obtained from the  $\text{Fe}(n, \gamma)$  reaction.  $\gamma$  lines denoted by P and F refer to photopeaks and first-escape peaks, respectively; other lines refer to double-escape peaks.

TMC analyzer. The full width at half maximum of a 6.0-MeV  $\gamma$  line was 9 keV for the 20-cc Ge(Li) detector and 10 keV for the 10-cc detector.

Angular-distribution measurements of the scattered spectrum were performed by mounting the detector on a rotating arm at a distance of 40 cm from the target. Typical running times were about 48 h for each angle. Time normalization at each angle was achieved by a preset number of counts in a 1.5-in.  $\times$  1.5-in. NaI detector which monitored the intensity of the direct  $\gamma$  beam. This detector was placed beyond a beam catcher through which a 1-mm hole was drilled for monitoring purposes. The variable energy response of the Ge(Li) detectors was calibrated with reference to the well-known intensities of the  $(n, \gamma)$  spectrum of chlorine

by employing the external thermal-neutron beam facility at IRR-2.

### III. RESULTS

#### A. Energy Spectrum and Identification of Scattering Isotope

The energy spectra of scattered photons from a La target as obtained by using the iron and titanium capture  $\gamma$  sources are shown in Figs. 1 and 2, respectively. About 6-mm thickness of lead was placed in front of the Ge(Li) detector for filtering out the large number of low-energy pulses obtained from atomic interactions of the direct  $\gamma$  beam with the scatterer. From Fig. 1 it may be seen that the scattered spectrum consists of three elastic compo-

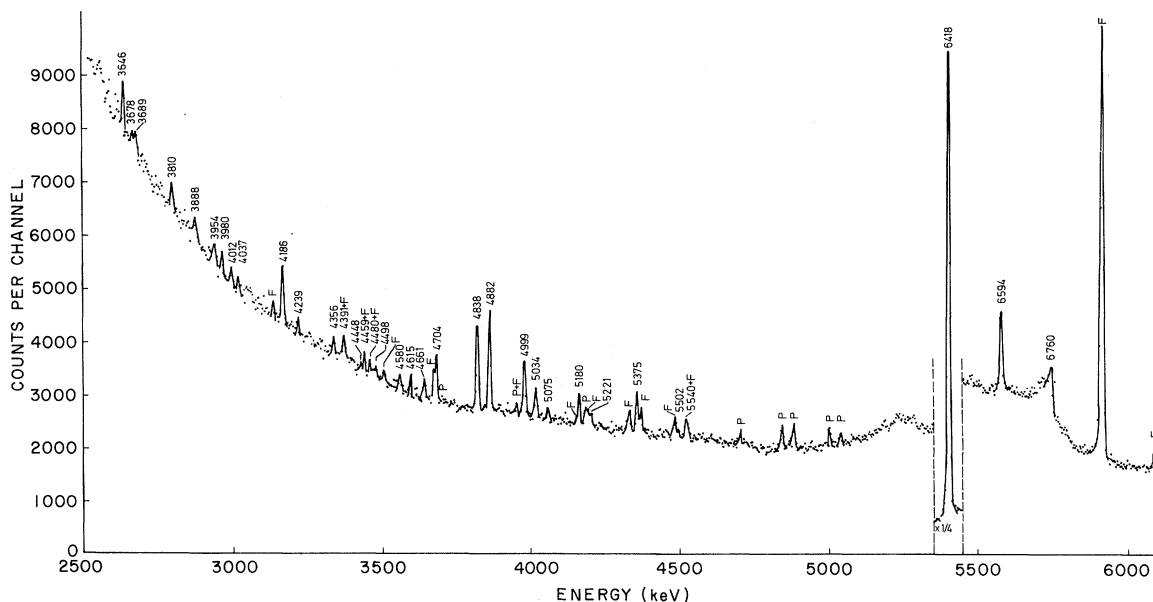


FIG. 2. Scattered  $\gamma$  spectrum from a La target at an angle of  $140^\circ$  measured by a 20-cc detector. The  $\gamma$  source was obtained from the  $\text{Ti}(n, \gamma)$  reaction.  $\gamma$  lines denoted by P and F refer to photopeaks and first-escape peaks, respectively; other lines refer to double-escape peaks.

nents at 7632, 7279, and 6018 keV, which correspond to strong-intensity lines in the  $\text{Fe}(n, \gamma)$  spectrum. Another line at 7158 keV seems to be due to elastic scattering of one of the neutron-capture  $\gamma$  lines of manganese. The capture  $\gamma$  rays of manganese have an intense line at 7159 keV which is known<sup>17</sup> to be resonantly scattered by  $^{139}\text{La}$ . In addition, manganese is expected to be present as an impurity in the iron  $\gamma$  source and to a larger extent in the stainless-steel holder of the  $\gamma$  source. All other lines in the scattered radiation spectrum correspond to inelastic transitions from the resonance levels to low-lying levels in  $^{139}\text{La}$ .

Figure 2 consists of two elastic components at 6418 and 6760 keV which correspond to strong-intensity lines in the  $\text{Ti}(n, \gamma)$  spectrum; the other lines in the scattered spectrum correspond to inelastic transitions between these resonance levels and low-lying levels in  $^{139}\text{La}$ .

It should be noted that natural La contains 99.911%  $^{139}\text{La}$  and 0.089%  $^{138}\text{La}$ . The contribution of  $^{138}\text{La}$  to the resonantly scattered spectrum is therefore expected to be negligible. In fact, none of the inelastically scattered lines were found to correspond to any known low-lying level in  $^{138}\text{La}$ . The scattering isotope in the present work was therefore taken to be  $^{139}\text{La}$ . Tables I and II list the results of line energies and relative intensities of scattered  $\gamma$  rays from a La target using neutron-capture  $\gamma$  sources of Fe and Ti, respectively.

#### B. Decay Scheme

In order to construct the decay scheme and hence,

TABLE I.  $\gamma$  energies of the scattered radiation from a La target; the  $\gamma$  source was obtained from the  $\text{Fe}(n, \gamma)$  reaction. The  $\gamma$ -line intensities were normalized relative to the 6018-keV line. Line energies are accurate to  $\pm 4$  keV.

$\gamma$ energy (keV)	Relative intensity
7632	3.0
7279	1.9
6018	100
5852	21.5
5699	1.3
5459	1.2
5360	2.0
5150	2.7
4798	14.4
4538	4.8
4481	5.8
4438	27.9
4334	13.6
4233	5.2
4062	1.1
3895	1.1

TABLE II.  $\gamma$  energies of the scattered radiation from a La target; the  $\gamma$  source was obtained from the  $\text{Ti}(n, \gamma)$  reaction. The  $\gamma$ -line intensities were normalized relative to the 6418-keV line. Line energies are accurate to  $\pm 4$  keV.

$\gamma$ energy (keV)	Relative intensity	$\gamma$ energy (keV)	Relative intensity
6760	1.8	4498	0.6
6594	4.8	4480	0.7
6418	100	(4459)	1.0
5540	3.1	4448	0.4
5502	2.9	4391	1.5
5375	2.3	4356	1.0
5221	1.0	4239	1.5
5180	1.3	4186	3.0
5075	0.7	4037	0.4
5034	1.9	4012	0.5
4999	3.1	3980	0.9
4882	5.0	3954	1.3
4838	4.4	3888	1.8
4704	1.8	3810	2.1
4661	1.2	3689	1.3
4615	1.1	3678	1.3
4580	0.9	3646	3.4

the energy levels of  $^{139}\text{La}$ , the independent resonance levels were first identified by comparing the scattered radiation spectrum with that of the incident  $\gamma$  beam. It was then assumed that all remaining high-energy  $\gamma$  lines are due to primary  $\gamma$  transitions deexciting the resonance levels. The majority of the high-energy  $\gamma$  lines were thus found to correspond to transitions to known low-lying levels in  $^{139}\text{La}$ .

The decay scheme in the present case is complex. The main difficulty is the excitation of more than one resonance level for each  $\gamma$  source used.

As mentioned earlier, no attempt was made to deduce new levels in the present work because of the ambiguity in associating a given  $\gamma$  transition with a specific resonance level. As a result, only transitions which were found to correspond to within 4 keV to known low-lying  $^{139}\text{La}$  levels were considered and included in the decay scheme; all other lines which did not fit to transitions to known low-lying levels were disregarded. Figure 3 shows the decay scheme obtained using the two  $\gamma$  sources of neutron capture in iron and titanium.

With the above procedure an ambiguity still remained with respect to three  $\gamma$  lines of energy 4999, 4838, and 4704 keV in the Ti  $\gamma$  source. These lines were found to fit to within 4 keV to the decay of both resonances at 6418 and 6760 keV to known low-lying levels in  $^{139}\text{La}$ . However, because of intensity considerations and partly because of the results of angular distributions, these three  $\gamma$  lines were taken to correspond to the



TABLE III. Level energies in  $^{139}\text{La}$  as obtained in the  $(\gamma, \gamma')$  reaction. Values obtained by other workers are also given.

Present work ( $\pm 4$ keV)	$\beta$ decay (Ref. a) (keV)	$(n, n')$ , $(n, n' \gamma)$ (Ref. b) (keV)
166	165.85 $\pm$ 0.02	166 $\pm$ 1
...	...	1206 $\pm$ 2
1220	1219.1 $\pm$ 0.4	1217 $\pm$ 1
1257	1256.6 $\pm$ 0.2	1255 $\pm$ 1
1384	1381.3 $\pm$ 0.5	1383 $\pm$ 2
1419	1420.5 $\pm$ 0.2	1420 $\pm$ 1
...	...	1439 $\pm$ 10
1480	1476.4 $\pm$ 0.3	1475 $\pm$ 2
1536	1536.3 $\pm$ 0.3	1538 $\pm$ 1
...	1558.2 $\pm$ 0.4	1559 $\pm$ 1
1580	1578.2 $\pm$ 0.4	1577 $\pm$ 1
1684	1683.1 $\pm$ 0.3	1682 $\pm$ 1
1714	...	1714 $\pm$ 2
1756 <sup>c</sup>	1761.1 $\pm$ 0.3	1756 $\pm$ 4
...	1765.5 $\pm$ 0.4	1768 $\pm$ 10
1820	...	1820 $\pm$ 4
1838	...	1835 $\pm$ 4
...	1857	1861 $\pm$ 9
1919	1920.6 $\pm$ 0.4	1929 $\pm$ 8
1956	1963	1959 $\pm$ 7
2061	2060.1 $\pm$ 0.4	2065 $\pm$ 7
2123	...	2124 $\pm$ 8
...	...	2198 $\pm$ 10
2232	...	2240 $\pm$ 12
...	...	2269 $\pm$ 15

<sup>a</sup>See Refs. 12 and 13.

<sup>b</sup>See Refs. 10 and 11.

<sup>c</sup>It is not clear whether this level is identifiable with the 1761.1-keV level.

decay of the 6418-keV resonance. The present conclusion regarding the 4704-keV line disagrees with that of Ref. 15 where it was assigned to the 6760-keV resonance. Table III summarizes the excitation energies of levels in  $^{139}\text{La}$  as obtained in the present work. The results reported by other workers are also given.

### C. Angular Distributions

Angular distributions of the intense lines in the scattered spectra were carried out using a 20-cc Ge(Li) detector. The scattering yield of each line was considered to be only the counts under the second-escape peak after subtracting a continuous background using a computer program. Corrections for the nuclear and atomic absorption of the incident beam and the atomic absorption of the scattered beam in the target scatterer were introduced. The experimental distribution of the elastically and strong inelastically scattered lines using the Fe- $(n, \gamma)$  and Ti- $(n, \gamma)$  sources are shown in Figs. 4 and 5, respectively. These distributions were fitted

with curves of the form  $W(\theta) = 1 + AP_2(\cos \theta)$  using the method of least squares.

The theoretical angular distribution of the scattered lines should be identical to that of a  $\gamma$ - $\gamma$  cascade of the form  $J_0 \rightarrow J \rightarrow J_f$  where  $J_0$ ,  $J$ , and  $J_f$  are the spins of the ground, resonance, and final states, respectively. Table IV lists the theoretical values of  $A$  corresponding to all possible  $\gamma$ - $\gamma$  cascades formed by pure dipole transitions in  $^{139}\text{La}$ . These values may be used for comparison with the experimental values and hence for deducing the spins of the levels. For mixed dipole-quadrupole transitions in which the resonance levels are assumed to be excited by pure dipole absorption, the angular distribution of the scattered radiation is given by

$$W(\theta) = A_0 + A_2 A_2' P_2(\cos \theta) \propto 1 + AP_2(\cos \theta),$$

where  $A_0 = 1 + x^2$ ,  $A_2 = a + 2bx + cx^2$ . The function  $P_2(\cos \theta)$  is a Legendre polynomial,  $x$  is the amplitude of quadrupole mixing ratio and  $a$ ,  $b$ ,  $c$ , and  $A_2'$  are the corresponding  $F$  coefficients<sup>18</sup> which depend on the spins of the states involved and on the multipolarity of the transition.

The assumption of pure dipole absorption was made after noting that the experimental distributions of the elastically scattered lines were identical (within the experimental error) to that of  $\gamma$ - $\gamma$  cascades involving pure dipole transitions (see below). Another argument in favor of this assumption is the fact that the character of the strong elastically scattered radiation is  $E1$ , as found by polarization measurements (see next section). It is expected, therefore, that all competing high-intensity transitions are  $E1$  and that the contribution of  $M2$  admixtures is very small. We hereby deal

TABLE IV. Theoretical values of the angular-distribution coefficients  $A$  for  $^{139}\text{La}$  corresponding to all possible  $\gamma$ - $\gamma$  cascades of the form  $\frac{J}{2} \rightarrow J \rightarrow J_f$ , where  $\frac{J}{2}$  is the spin of the  $^{139}\text{La}$  ground state; pure dipole transitions are assumed.

$J$	$J_f$	$A$
$\frac{5}{2}$	$\frac{3}{2}$	0.050
$\frac{5}{2}$	$\frac{5}{2}$	-0.057
$\frac{5}{2}$	$\frac{7}{2}$	0.018
$\frac{7}{2}$	$\frac{5}{2}$	-0.143
$\frac{7}{2}$	$\frac{7}{2}$	0.190
$\frac{7}{2}$	$\frac{9}{2}$	-0.067
$\frac{9}{2}$	$\frac{7}{2}$	0.092
$\frac{9}{2}$	$\frac{9}{2}$	-0.133
$\frac{9}{2}$	$\frac{11}{2}$	0.050

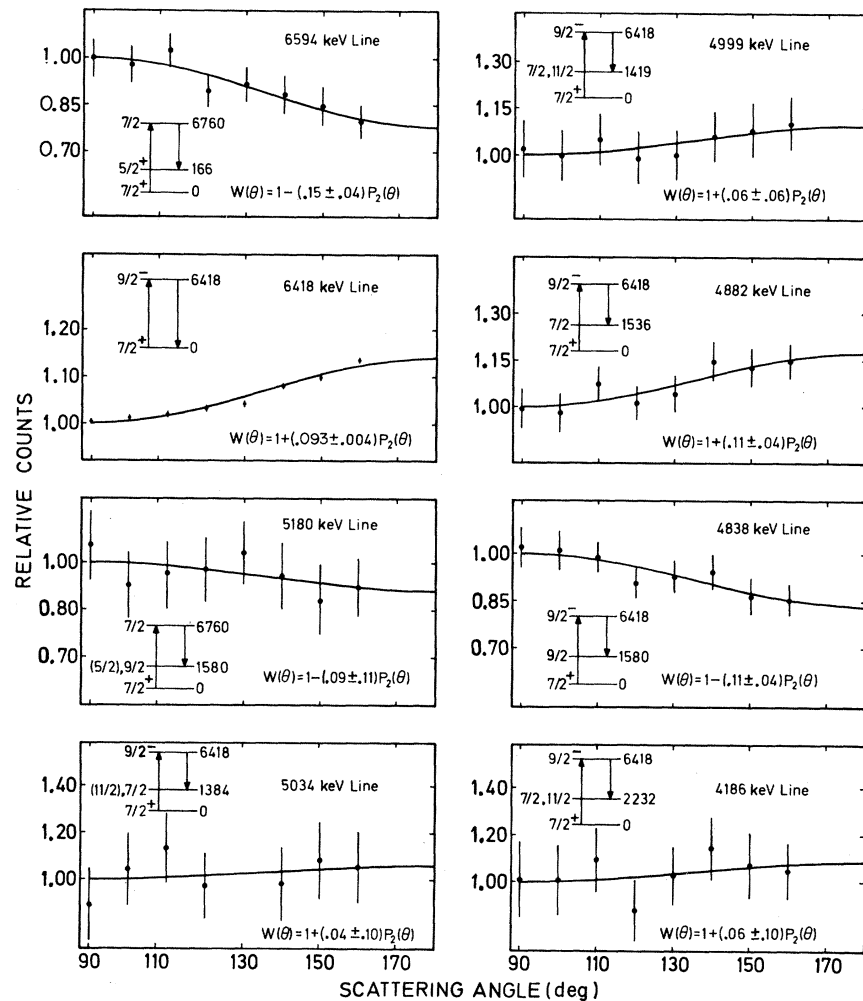


FIG. 5. Angular distributions of some intense  $\gamma$  lines scattered by  $^{139}\text{La}$  using a  $\gamma$  source obtained from the  $\text{Ti}(n, \gamma)$  reaction. See caption to Fig. 4.

with the  $^{139}\text{La}$  levels that were strongly populated in the present experiment.

#### 1. 6018-, 6418-, and 6760-keV Levels

The 6018-keV level was excited by the  $\text{Fe}(n, \gamma)$  source. By comparing the experimental and theoretical values (Tables IV and V) of the angular-distribution coefficients  $A$  of the 6018-keV line, it was found that the spin of the 6018-keV level is  $\frac{7}{2}$ . In a similar manner, the spin of the 6418-keV level may be seen to be  $\frac{9}{2}$ . These results combined with the  $E1$  character of these lines (see below) indicates that the parities of these two levels are odd.

The  $M2/E1$  mixing ratios were obtained by plotting the theoretical value of  $A$  as a function of  $x$ , and comparing with the experimental value of  $A$ . The values of  $x$  (listed in Table V) for these two transitions were found to be small, which justifies the assumption of pure dipole absorption.

The 6760-keV level was weakly excited using the  $\text{Ti}(n, \gamma)$  source and it was impossible to measure the angular distribution with good accuracy. The

spin of this level was, however, inferred from the experimental distribution of the relatively strong 6594-keV line which corresponds to the decay of the 6760-keV resonance to the 166-keV level in  $^{139}\text{La}$ . The spin of the 166-keV level was found to be  $\frac{5}{2}$  (see below) and the experimental distribution of the 6594-keV line was found to agree with the sequence  $\frac{7}{2}(1)\frac{7}{2}(1)\frac{5}{2}$ . This fixes the spin of the 6760-keV level as  $\frac{7}{2}$ . The possibility of quadrupole admixture was considered by plotting  $A$  as a function of  $x$  for the 6594-keV level and for two assumed spin possibilities of the 6760-keV level (Fig. 6). It is clear from the figure that the only possible spin for the 6760-keV resonance is  $\frac{7}{2}$  and that the quadrupole-dipole mixing amplitude in the 6594-keV transition is small (Table V). Here it was assumed that all inelastic transitions are predominantly  $E1$ .

#### 2. 166-keV Level

This line was populated independently by the 5852- and 6594-keV lines from the two resonanc-

TABLE V. Most probable spins and parities of levels in  $^{139}\text{La}$  as found in the present work. Also listed are the corresponding  $\gamma$ -line energies, the experimental angular-distribution coefficients  $A$ , and the  $M2/E1$  mixing amplitudes  $x$ . The values of  $x$  are given for more than one possible spin value. The 1580-keV level was populated by more than one resonance. Parentheses indicate uncertainties.

Level energy (keV)	Spin and parity	$\gamma$ -line energy (keV)	$A \pm \Delta A$	$x$ ( $M2/E1$ ) <sup>a</sup>
6760	$\frac{7}{2}(-)$	6594	$-0.15 \pm 0.04$	$-0.013 \pm 0.056$
6418	$\frac{9}{2}^-$	6418	$0.093 \pm 0.004$	$-0.001 \pm 0.004$
6018	$\frac{7}{2}^-$	6018	$0.17 \pm 0.02$	$-0.01 \pm 0.03$
166	$\frac{5}{2}^+$	5852	$-0.16 \pm 0.04$	$-0.02 \pm 0.06$
1220	$\frac{5}{2}$	4798	$-0.15 \pm 0.08$	$-0.03 \pm 0.08$
1220	$(\frac{9}{2})$	4798	$-0.15 \pm 0.08$	$0.15 \pm 0.10$
1384	$\frac{7}{2}$	5034	$0.04 \pm 0.10$	$0.10 \pm 0.18$
1419	$\frac{7}{2}$	4999	$0.06 \pm 0.06$	$0.06 \pm 0.12$
1419	$(\frac{11}{2})$	4999	$0.06 \pm 0.06$	$0.02 \pm 0.14$
1536	$\frac{7}{2}$	4882	$0.11 \pm 0.04$	$-0.03 \pm 0.08$
1580	$\frac{9}{2}$	4838	$-0.11 \pm 0.04$	$-0.09^{+0.29}_{-0.19}$
1580	$\frac{9}{2}$	4438	$-0.07 \pm 0.09$	$0.005 \pm 0.115$
1580	$\frac{9}{2}$	5180	$-0.09 \pm 0.11$	$0.03 \pm 0.18$
1580	$(\frac{5}{2})$	5180	$-0.09 \pm 0.11$	$0.07 \pm 0.14$
2232	$\frac{7}{2}$	4186	$0.06 \pm 0.10$	$0.07 \pm 0.18$
2232	$(\frac{11}{2})$	4186	$0.06 \pm 0.10$	$0.01 \pm 0.23$

<sup>a</sup>Here it was tacitly assumed that all transitions are predominantly  $E1$ .

es at 6018 and 6760 keV, respectively. The angular distribution of the 5852-keV line (Fig. 4) was found to agree with that corresponding to the sequence  $\frac{7}{2}(1)\frac{7}{2}(1)\frac{5}{2}$ , thus fixing the spin of the 166-keV level to be  $\frac{5}{2}$ . The value of the quadrupole-dipole mixing amplitude was obtained by the same method discussed above and is given in Table V. The character of the 5852-keV transition is expected to be  $E1$  because its radiation strength  $I_\gamma/E_\gamma^3$  is of about the same magnitude as that of the 6018-keV ground-state  $E1$  transition. The 166-keV level should therefore be  $\frac{5}{2}^+$  in agreement with previous results.<sup>12</sup> As expected, no transition was observed between the 6418-keV  $\frac{9}{2}^-$  level and the 166-keV  $\frac{5}{2}^+$  level, because this involves an  $M2$  transition which is very unlikely to occur.

### 3. 1220-keV Level

This level was strongly populated by the 4798-keV line from the 6018-keV resonance. Its corresponding angular distribution was found to be in

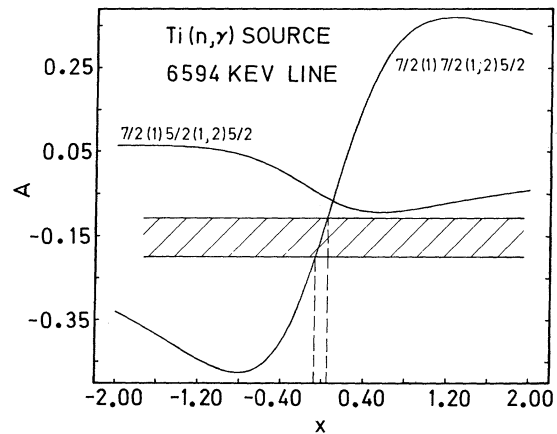


FIG. 6. A plot of the angular-distribution coefficient  $A$  as a function of the mixing ratio  $x$  for the sequence  $\frac{7}{2}(1)\frac{7}{2}(1,2)\frac{5}{2}$  and  $\frac{7}{2}(1)\frac{5}{2}(1,2)\frac{5}{2}$ . The figure indicates the allowed values of  $x$  for the 6594-keV transition only.

better agreement with a spin assignment of  $\frac{5}{2}$  than a spin of  $\frac{9}{2}$ . The quadrupole-dipole mixing amplitude for each of these two possible spins was also calculated (Table V) and again favors a  $\frac{5}{2}$  assignment. It may be noted that the 1220-keV level was populated from the  $\frac{7}{2}$  6760-keV resonance, and no transition was observed from the  $\frac{9}{2}^-$  6418-keV resonance. These facts favor a  $\frac{5}{2}$  assignment to the 1220-keV level. Nevertheless, a  $\frac{9}{2}$  assignment cannot entirely be excluded.

### 4. 1384-keV Level

This level was populated by the 5034- and 5375-keV transitions corresponding to the 6418- and 6760-keV resonances. Since the spins of these resonances are  $\frac{9}{2}$  and  $\frac{7}{2}$ , and because only dipole transitions are expected to be observed in this experiment, the possible spins of the 1384-keV level are therefore  $\frac{7}{2}$  and  $\frac{9}{2}$ . However, the only spin values consistent with the angular distribution of the 5034-keV line were  $\frac{7}{2}$  and  $\frac{11}{2}$ , with a higher preference to  $\frac{7}{2}$  (Fig. 4). Combining both results, it may be concluded that the spin of the 1384-keV level is  $\frac{7}{2}$ . The corresponding transition from the resonance state is probably not pure dipole. The amount of quadrupole admixture was calculated and is given in Table V.

### 5. 1419-keV Level

This level was populated by the 4999-keV transition from the 6418-keV resonance. Its angular distribution is consistent with both  $\frac{7}{2}$  and  $\frac{11}{2}$  spin assignments. It is not entirely evident which level the 1419-keV line found here should be identified with. In the literature,<sup>12,13</sup> a level at 1420.5 keV was reported through the study of the decay of

$^{139}\text{Ba}$ . In addition, a level at 1.42 MeV was reported by Wildenthal, Newman, and Auble (WNA)<sup>14</sup> by studying the  $^{138}\text{Ba}(^3\text{He}, d)$  reaction; it was assigned a  $J^\pi$  value of  $\frac{11}{2}^-$  and is reported to be the  $h_{11/2}$  single-proton state in  $^{139}\text{La}$ . In addition, Malan *et al.*<sup>10</sup> report the existence of two levels at 1420 and 1439 keV through the use of the  $(n, n')$  technique. It appears that the 1.42-MeV level of WNA may be identified with the 1439-keV level of Malan *et al.*, and the 1419-keV level found in the present work is identifiable with the 1420.5-keV level found in  $^{139}\text{Ba}$  decay<sup>12, 13</sup> and the  $(n, n')$  reaction.<sup>10</sup>

Since this level was found to decay<sup>12, 13</sup> to the ground-state  $\frac{7}{2}^+$  and the 166-keV  $\frac{5}{2}^+$  levels, it means that an  $\frac{11}{2}$  assignment for the 1419-keV level may be excluded and therefore the only possible spin value left is  $\frac{7}{2}$ .

#### 6. 1536-keV Level

This level was populated via the three resonance levels at 6018, 6418, and 6760 keV. Its spin should therefore be either  $\frac{7}{2}$  or  $\frac{9}{2}$ . In fact, the angular distribution of the 4882-keV line leading to this level was found to be consistent with a  $\frac{7}{2}$  spin (Fig. 3) with a small quadrupole-dipole mixing amplitude (Table V). The spin of this level is therefore  $\frac{7}{2}$  because a  $\frac{9}{2}$  assignment would require a quadrupole admixture of about 100%.

#### 7. 1580-keV Level

This level was populated by the three resonance levels at 6018, 6418, and 6760 keV. The spin of this level should therefore be either  $\frac{7}{2}$  or  $\frac{9}{2}$ . The angular distributions of the 4838- and 4438-keV lines leading to this level were measured and are both consistent with a spin assignment of  $\frac{9}{2}$  and  $\frac{5}{2}$  with a higher preference to  $\frac{9}{2}$ . Combining the above results it may be concluded that the spin of the 1580-keV level is  $\frac{9}{2}$ . The possible quadrupole-dipole amplitude for each case was calculated and is given in Table V.

#### 8. 2232-keV Level

This level was populated by the 4186-keV line from the 6418-keV resonance. The angular distribution is consistent with spin values of  $\frac{7}{2}$  and  $\frac{11}{2}$  to the 2232-keV level.

#### D. Parities of Resonance Levels

The parities of the strongly excited resonance levels were established by measuring the polarization of the elastically scattered photons using a Compton polarimeter.<sup>19</sup> The degree of polarization to be expected for elastically scattered radiation is identical to that of a  $\gamma$ - $\gamma$  cascade of the

form  $J_0 - J \rightarrow J_0$ .

The theoretical expression of the polarization for the general case of a mixed dipole-quadrupole transition, and also the experimental details of the measurement were given in a previous publication.<sup>20</sup> Here, we only mention that the polarimeter consisted of a central NaI detector which served as a Compton scatterer, and a second NaI crystal for coincidence detection of the scattered radiation. This second crystal could be set in two positions, parallel and perpendicular to the scattering plane. The sum-coincidence spectrum for the elastically scattered radiation at 6418 keV (obtained with a Ti  $\gamma$  source) corresponding to the two perpendicular planes is shown in Fig. 7. A similar sum-coincidence spectrum was obtained for the 6018-keV resonance line (not shown) using a La scatterer and Fe  $\gamma$  source. The ratio of the number of coincidences in the perpendicular and parallel planes as determined from the photopeaks of the lines are

$$\frac{N_{\perp}}{N_{\parallel}}(6018) = 0.960 \pm 0.008, \quad \frac{N_{\perp}}{N_{\parallel}}(6418) = 0.981 \pm 0.007,$$

which indicate that the elastic radiation in both cases is E1. Therefore, the parities of the two resonance levels at 6018 and 6418 keV are odd. It is interesting to note that these values of  $N_{\perp}/N_{\parallel}$  are exactly equal to the theoretical values for pure E1, obtained by accounting for the spins in question and for the finite geometry of the polarimeter.<sup>20</sup>

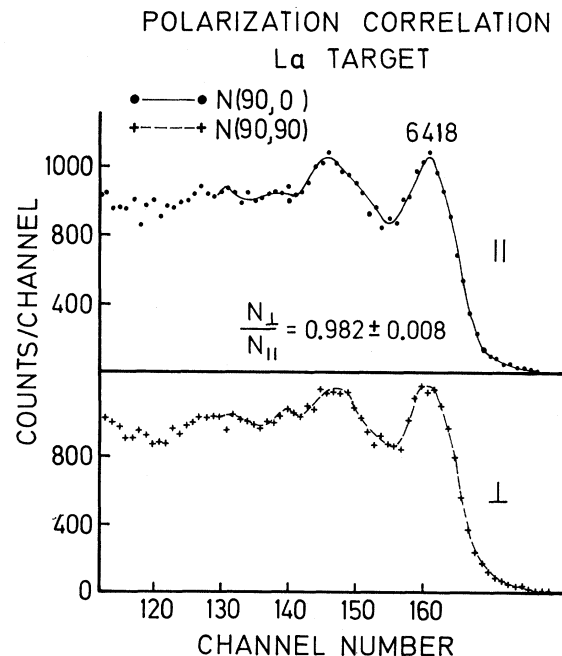


FIG. 7. Sum-coincidence spectra obtained with the NaI detectors in planes perpendicular ( $\perp$ ) and parallel ( $\parallel$ ) to the resonance scattering plane.  $N_{\perp}$  and  $N_{\parallel}$  refer to the area under the photopeaks.



Because of the dominant intensity of the 6418-keV line in the scattered radiation spectrum and the intrinsically low resolution of NaI detectors, all other lines of the scattered radiation did not show up clearly in the sum-coincidence spectrum. In particular, it was not possible to measure the parity of the weakly excited 6760-keV resonance level.

#### E. Branching Ratios, Radiative Widths, and Scattering Cross Sections

The branching ratios for the decay of the 6418- and 6018-keV levels were evaluated from the relative intensities of the scattered  $\gamma$  lines as measured at a certain angle after accounting for the angular distributions of the lines deexciting each resonance level. The results are given in Fig. 3. No branching ratios are given for the other weak resonance levels, because some of the corresponding inelastic lines are expected to have been missed in the present measurement.

In a previous publication,<sup>20</sup> it was noted that in order to determine the radiative width of a resonance level in a resonance scattering process, one has to measure the four parameters involved. These are, the spin  $J$  of the resonance, the ground-state radiative width  $\Gamma_0$ , the total radiative width  $\Gamma_\gamma$ , and the distance  $\delta$  between the peaks of the incident-energy line and the resonance level. The measurement of  $J$  and  $\Gamma_0/\Gamma_\gamma$  was mentioned above. Another two experiments, namely, a temperature variation measurement and a self-absorption experiment,<sup>20</sup> are necessary to determine  $\Gamma_0$  and  $\delta$ . For checking the consistency of these parameters another experiment was performed in which the effective elastic cross section  $\langle\sigma_r\rangle$  for elastic scattering was measured and was compared with the calculated value of  $\langle\sigma_r\rangle$  which is a function of all parameters of the resonance level. For cases where no agreement was obtained, it was found necessary to vary the values of  $\Gamma_0$ ,  $\Gamma_0/\Gamma_\gamma$ , and  $\delta$  within the limits of experimental errors so as to get agreement between the two values of  $\langle\sigma_r\rangle$ . It was noted<sup>20</sup> that this consistency check is a prerequisite for a reliable experimental result of  $\Gamma_\gamma$ . Measurements performed without such a check may yield different values. This is the reason for the discrepancies in the values of  $\Gamma_\gamma$  as reported here and in that obtained without this check.<sup>15, 16</sup>

The values of the parameters which best fitted all experiments were

$$\begin{aligned} 6018 \text{ keV: } & \Gamma_\gamma = 0.051_{-0.006}^{+0.014} \text{ eV}, & \Gamma_0/\Gamma_\gamma &= 0.5, \\ & \langle\sigma_r\rangle = 39 \text{ mb}, & \delta &= 8.2 \pm 0.6 \text{ eV}; \\ 6418 \text{ keV: } & \Gamma_\gamma = 0.081_{-0.007}^{+0.013} \text{ eV}, & \Gamma_0/\Gamma_\gamma &= 0.78, \\ & \langle\sigma_r\rangle = 142 \text{ mb}, & \delta &= 9.5 \pm 0.5 \text{ eV}. \end{aligned}$$

The values of  $\langle\sigma_r\rangle$  are at a  $\gamma$ -source temperature of 380°C and a target temperature of 25°C.

## IV. DISCUSSION

### A. Energy Levels of <sup>139</sup>La

The <sup>139</sup>La nucleus consists of 82 neutrons forming a closed shell and 57 protons. The seven protons outside the  $Z=50$  closed shell fill the  $g_{7/2}$  and  $d_{5/2}$  orbits. Other available orbits are  $3s_{1/2}$ ,  $2d_{3/2}$ , and  $1h_{11/2}$ , which lie about 1 MeV or so higher in energy. The energy levels of <sup>139</sup>La were calculated by Wildenthal<sup>21</sup> using the shell model and a modified surface  $\delta$  interaction. In this calculation, six of the protons which are outside the  $Z=50$  shell were allowed to occupy the  $g_{7/2}$ - $d_{5/2}$  configuration space while the remaining proton was placed in either the  $3s_{1/2}$  or  $2d_{3/2}$  orbit. No negative-parity states were incorporated in the calculations. The single-particle energies and the strengths of the surface  $\delta$  interaction and the modifying term were taken from experiment by least-squares fitting to known energy levels in  $N=82$  nuclei. The result yielded a large number of even-parity states in the energy range 1.14 and 2.53 MeV with spin values between  $\frac{1}{2}$  and  $\frac{15}{2}$ .

It is impossible to make any detailed comparison between the predicted levels and experiment because the spins of only four levels in the energy region between 1.14 and 2.53 MeV were determined with certainty. It is interesting, however, to make a gross-feature comparison between theory and experiment. Such a comparison is possible only under the assumption that all low-lying levels populated in the present work are of even parity. It may be noted that the levels detected in the present experiment should have one of the spin values  $\frac{3}{2}$ ,  $\frac{7}{2}$ ,  $\frac{9}{2}$ , or  $\frac{11}{2}$ . The total number of these levels is 17, while the total number of predicted levels having the same spin values and positive parity is also 17. This agreement is probably accidental because several other levels in the same energy range is expected to have been missed in the present experiment. Nevertheless, the above comparison indicates that the shell-model description of the <sup>139</sup>La energy levels by Wildenthal is in much better accord with experiment than that of Freed and Miles<sup>22</sup> who employed the unified model for their calculation.

### B. Quadrupole-Dipole Mixing Ratios

Angular-correlation measurements in  $\gamma$ - $\gamma$  cascades may in general be used to study the purity of the character of electromagnetic transitions. The angular-distribution measurements of the present work, while intended primarily to measure the

spin values of energy levels in  $^{139}\text{La}$ , may also be used for studying the quadrupole-dipole mixing ratios in high-energy transitions in  $^{139}\text{La}$ . The results of linear-polarization measurements can decide about the dominant character of the radiation and are not very sensitive to small amounts of quadrupole admixtures. In the present work, the elastic transitions for two strong resonances were found to be of predominantly  $E1$  character. The most refined result of the amount of the  $M2$  admixture was obtained for the case of the 6418-keV line,  $\alpha^2 < 2.5 \times 10^{-5}$ . The intensity of this line was very strong and the accuracy of the measurement was relatively high (Fig. 4). For all other transitions observed in the present work, the measurement of angular distribution was less accurate and the uncertainty in the value of  $M2/E1$  was correspondingly higher (Table V).

According to the single-particle Moszkowski estimate,<sup>23</sup> the ratio of the single-particle widths of

$M2$  and  $E1$  transitions as reported by Wilkinson<sup>24</sup> is given by

$$\frac{\Gamma(M2)}{\Gamma(E1)} = 8.1 \times 10^{-7} E_{\gamma}^2 = 3.3 \times 10^{-5},$$

which is of about the same magnitude as that of the measured value for the 6418-keV transition. The above measurement does not constitute, however, an experimental check of the ratio of the single-particle  $E1$  and  $M2$  strengths. This is because these strengths are expected to be fragmented among a large number of levels, each of which is deexcited by several inelastic transitions. A proper experimental check would mean a measurement of the  $M2/E1$  mixing ratio of each transition separately. This necessitates higher incident  $\gamma$ -ray beam intensities, which may enable the performance of angular-distribution measurements of higher precision.

- 
- <sup>1</sup>R. Moreh and A. Nof, Phys. Rev. 178, 1961 (1969).  
<sup>2</sup>R. Moreh and A. Wolf, Phys. Rev. 182, 1236 (1969).  
<sup>3</sup>R. Moreh and O. Shahal, Phys. Rev. 188, 1765 (1969).  
<sup>4</sup>G. P. Estes and K. Min, Phys. Rev. 154, 1104 (1967).  
<sup>5</sup>V. E. Michalk and J. A. McIntyre, Nucl. Phys. A137, 115 (1969).  
<sup>6</sup>R. Cesareo *et al.*, Nucl. Phys. A132, 512 (1969).  
<sup>7</sup>Y. Schlesinger, M. Hass, B. Arad, and G. Ben-David, Phys. Rev. 178, 2013 (1969).  
<sup>8</sup>N. Shikazono and Y. Kawarasaki, Nucl. Phys. A118, 114 (1968).  
<sup>9</sup>J. M. Daniels and J. Felsteiner, Can. J. Phys. 46, 1849 (1968).  
<sup>10</sup>J. G. Malan *et al.*, Nucl. Phys. A124, 111 (1969).  
<sup>11</sup>P. Van Der Merwe *et al.*, Nucl. Phys. A124, 433 (1969).  
<sup>12</sup>J. C. Hill and M. L. Wiedenbeck, Nucl. Phys. A119, 53 (1968).  
<sup>13</sup>G. Berzins, M. E. Bunker, and J. W. Starner, Nucl. Phys. A128, 294 (1969).  
<sup>14</sup>B. H. Wildenthal, E. Newman, and R. L. Auble, Phys. Letters 27B, 628 (1968).  
<sup>15</sup>H. Szichman, Y. Schlesinger, G. Ben-David, and D. Pavel, to be published.  
<sup>16</sup>R. Moreh and A. Nof, in *Proceedings of the International Symposium on Neutron Capture Gamma-Ray Spectroscopy, Studsvik, Sweden, 1969* (International Atomic Energy Agency, Vienna, Austria, 1969). This article contains an error; the 6018-keV transition is  $E1$  and not  $M1$ .  
<sup>17</sup>G. Ben-David, B. Arad, J. Balderman, and Y. Schlesinger, Phys. Rev. 146, 852 (1966).  
<sup>18</sup>M. Ferentz and N. Rosenzweig, in *Alpha-, Beta-, and Gamma-Ray Spectroscopy*, edited by K. Seigbahn (North-Holland Publishing Company, Amsterdam, The Netherlands, 1966), p. 1687.  
<sup>19</sup>F. Metzger and M. Deutsch, Phys. Rev. 78, 551 (1950).  
<sup>20</sup>R. Moreh, S. Shlomo, and A. Wolf, Phys. Rev. C 2, 1141 (1970).  
<sup>21</sup>B. H. Wildenthal, Phys. Rev. Letters 22, 1118 (1969); and private communication.  
<sup>22</sup>N. Freed and W. Miles, Nuovo Cimento 60, 30 (1969).  
<sup>23</sup>S. A. Moszkowski, in *Alpha-, Beta-, and Gamma-Ray Spectroscopy*, edited by K. Seigbahn (North-Holland Publishing Company, Amsterdam, The Netherlands, 1966), p. 863.  
<sup>24</sup>D. H. Wilkinson, in *Nuclear Spectroscopy*, edited by F. Ajzenberg-Selove (Academic Press Inc., New York, 1960), Pt. B, p. 852.